



Cometabolic removal of organic micropollutants by enriched nitrite-dependent anaerobic methane oxidizing cultures

Miguel Martínez-Quintela, Adrián Arias, Teresa Alvarino, Sonia Suarez, Juan Manuel Garrido, Francisco Omil

Accepted Manuscript

How to cite:

Journal of Hazardous Materials, 402 (2021), 123450. doi: 10.1016/j.jhazmat.2020.123450

Copyright information:

© 2020 Elsevier B.V. This manuscript version is made available under the CC-BY-NC-ND 4.0 license (<http://creativecommons.org/licenses/by-nc-nd/4.0>)

1 **Cometabolic removal of organic micropollutants by enriched nitrite-**
2 **dependent anaerobic methane oxidizing cultures**

3

4 Miguel Martínez-Quintela^{1,*}, Adrián Arias¹, Teresa Alvariño^{1,2}, Sonia Suárez¹, Juan
5 Manuel Garrido¹ and Francisco Omil¹.

6

7 ¹Department of Chemical Engineering, School of Engineering, University of Santiago de
8 Compostela, Campus Vida, E-15782, Santiago de Compostela, Spain

9 ²Galician Water Research Center Foundation (Cetaqua Galicia). Emrendia Building,
10 University of Santiago de Compostela, Campus Vida, E-15782, Santiago de Compostela,
11 Spain

12

13 ***Corresponding author:** Miguel Martínez-Quintela. E-mail: m.martinez.quintela@usc.es

14

15

16

17

18

19 **Abstract**

20 The innovative and recently discovered n-damo process, based on anaerobic methane
21 oxidation with nitrite, was developed in a membrane-based bioreactor and evaluated in terms
22 of organic micropollutants (OMPs) removal. The main singularity of this study consisted in
23 the evaluation of organic micropollutants (OMPs) removal in the biological reactor. A
24 strategy consisting on progressively increasing the nitrogen loading rate in order to increase
25 the specific denitrification activity was followed to check if the selected OMPs were co-
26 metabolically biotransformed. Significant nitrite removal rate ($24.1 \text{ mg N L}^{-1} \text{ d}^{-1}$) was
27 achieved after only 30 days of operation. A maximum specific removal of $186.3 \text{ mg N gVSS}^{-1}$
28 d^{-1} was obtained at the end of the operation, which is one of the highest previously reported.
29 A successfully n-damo bacteria enrichment was achieved, being *Candidatus*
30 *Methylomirabilis* the predominant bacteria during the whole operation attaining a maximum
31 relative abundance of about 40%. The natural hormones (E1 and E2) were completely
32 removed in the bioreactor. The specific removal rates of erythromycin (ERY), fluoxetine
33 (FLX), roxithromycin (ROX) and sulfamethoxazole (SMX) were successfully correlated
34 with the specific nitrite removal rates, suggesting a co-metabolic biotransformation.

35

36 **Keywords:** n-damo process, organic micropollutants, cometabolism, enrichment, MBR

37

38

39

40

41

42

43 1. INTRODUCTION

44 Anaerobic wastewater treatment processes have been largely applied in areas with temperate
45 and warm climates due to their lower energy consumption, generation of an enriched-
46 methane biogas and lower biomass production, relative to conventional aerobic systems. The
47 generated effluents can pose an environmental problem due to their high ammonia
48 concentration, and their significant content in dissolved methane, which is very often directly
49 desorbed into the atmosphere (Noyola et al., 2006; Souza et al., 2011).

50 Conventional biological nitrogen removal process has been applied to urban wastewater in
51 order to reduce water eutrophication in downstream water bodies. The main drawbacks of
52 this process (as requirement of a biodegradable carbon source, high energy consumption,
53 sludge production and greenhouse gas emissions) can be addressed with novel treatment
54 processes, such as those based on autotrophic anaerobic ammonium oxidation (anammox),
55 combined with nitrite/nitrate dependent anaerobic methane oxidation (n-damo), which have
56 proven to reduce effectively nitrogen from wastewater economically and with less
57 environmental impact (Liu et al., 2019).

58 The recently discovered n-damo bacteria (*Candidatus Methyloirabilis* Species: *M. oxyfera*;
59 *M. sinica*; *M. lanthanidiphila*), bacteria affiliated with the NC10 phylum, have demonstrated
60 their ability to perform both nitrogen and methane removal, by anaerobically oxidizing
61 methane using nitrite as electron acceptor (Ettwig et al., 2010; He et al., 2016; Versantvoort
62 et al., 2018). The slow growth of this microorganism, between 1 and 2 weeks, implies that
63 the enrichment process of this bacteria in a mixed culture may take several months (Allegue

64 et al., 2018; Ettwig et al., 2009). Thus, in order to avoid problems related with biomass
65 washout, n-damo bacteria enrichments have been successfully achieved using membrane
66 bioreactor-based configurations (MBR). Among the first results using this type of
67 configuration were those reported by Kampman et al. (2014) achieving a nitrite removal rate
68 of 36 mg N L⁻¹ d⁻¹. After further development, these results could be improved to nitrite
69 removal rates of 116 mg N L⁻¹ d⁻¹ by Allegue et al. (2018).

70 N-damo microorganisms (bacteria and archaea) are currently object of interest because of
71 their suitability to develop innovative processes in which methane and nitrogen compounds
72 can be simultaneous removed. Additionally, previous studies showed positive results at pilot
73 scale hybrid (anoxic-aerobic) reactors for the removal of organic micropollutants (OMPs)
74 (Arias et al., 2018). However, until now, the n-damo based technology is not suitable for its
75 implementation in WWTPs since it is not possible to achieve high denitrification activities
76 (Wang et al., 2017). Thus, more research about is needed to enhance their metabolic activity
77 as well as to analyze the possible effects on their development in the presence of other
78 substances like OMPs.

79 OMPs are currently considered as an important challenge to be addressed by the new
80 innovative technology developed, since they have been linked with several environmental
81 risks (Tran et al., 2018). The European Union started to advance in the regulation of these
82 contaminants in water (Sousa et al., 2018), by the establishment of a watchlist that identifies
83 8 compounds that should be monitored (last updated by Commission decision (EU) 2018/840
84 of 5 June 2018). It included in 2015 three macrolide antibiotics - erythromycin, azithromycin
85 and clarithromycin; three hormones – estrone, estradiol and ethinylestradiol; one anti-
86 inflammatory drug – diclofenac (DCF). Its update 2018 supposed among others the

87 incorporation of two additional antibiotics: amoxicillin (group of penicillins) and
88 ciprofloxacin (group of quinolones), as well as the removal of DCF.

89 Among the different factors which determine OMP removal in biological reactors, the redox
90 conditions have shown to highly influence their fate. Depending on the condition applied,
91 different microbial populations will grow, activating different metabolic routes and enzymes
92 and, consequently, determining the biotransformation route of the micropollutant. In general,
93 removal efficiencies are larger in aerobic conditions compared to anoxic ones, due to the
94 higher oxidation potential of the oxygen compared with NO_x species (Alvarino et al., 2018).
95 The combination of different redox environments normally maximizes the final removal
96 efficiency (Arias et al., 2018). A lack of knowledge on the OMP biotransformation in anoxic
97 environments is still identified (Torresi et al., 2017).

98 OMPs are commonly present at trace levels in water bodies. Consequently, cometabolism is
99 considered as the main biotransformation mechanism, in which the presence of a growth
100 substrate is needed to promote the production of non-specific enzymes which can
101 accidentally biotransform OMPs (Fischer and Majewsky, 2014; Plosz et al., 2010; Tran et
102 al., 2013). One of the most studied cometabolic processes are linked to nitrification, in which
103 the ammonium monooxygenase enzyme has proven to have an active role on several OMP
104 biotransformation due to its low specificity (Fernandez-Fontaina et al., 2016). Under anoxic
105 environments, Polesel et al. (2017) found positive correlations between the specific
106 heterotrophic denitrifying activity and the biotransformation rate constants of different non-
107 recalcitrant compounds. Until now, few studies about cometabolism were performed under
108 anaerobic or anoxic environments (Gonzalez-Gil et al., 2019; Pomiès et al., 2015). As far as

109 the authors know, there are neither previous studies about OMP removal in processes based
110 on the use of n-damo microorganisms.

111 The aim of this study was to achieve an enriched n-damo bacteria culture in an MBR-based
112 configuration and to assess the removal efficiency of OMPs in the system. The research was
113 focused on monitoring the reactor performance at increasing nitrogen loading rates in order
114 to evaluate the robustness of the system in terms of conventional parameters and bacterial
115 dynamics. Besides, the cometabolic biotransformation of OMPs was assessed by studying
116 the correlations between the denitrification kinetics and the OMP removal rates.

117 **2. MATERIALS AND METHODS**

118 **2.1 Reactor configuration and operation**

119 A 10 L lab-scale MBR was used to carry out the enrichment of n-damo culture, with a
120 working volume of 6.65 L (Fig. S1). Due to low activities of these microorganisms, complete
121 biomass retention in the reactor was achieved by using a submerged hollow-fiber
122 ultrafiltration membrane module (Puron), which was operated in cycles of 7 min of
123 permeation and 0.5 min of relaxation. The surface of the membrane was 0.5 m² and the pore
124 size 0.03 μm. A pressure sensor PN2069 (IFM) was used to record permeation and relaxation
125 transmembrane pressures and an Atlas Scientific pH Probe was placed inside the reactor. The
126 reactor was provided with a thermostatic bath to maintain the temperature at 28 °C.

127 The inoculum used was taken from a denitrifying pre-anoxic MBR treating an UASB
128 effluent, in which dissolved methane was used as carbon source for denitrification (Silva-
129 Teira et al., 2017). This biomass was composed of a complex microbial population and
130 characterized by a low presence of n-damo bacteria. A total suspended solids concentration

131 of 0.5 g L⁻¹ was used as inoculum. The system was fed with a medium containing 9 mg L⁻¹
132 of NH₄Cl, 100 mg L⁻¹ of NaHCO₃ and NaNO₂ as nitrite source according to biomass activity
133 capacity and requirements for this study. The addition of ammonium nitrogen was decided
134 according to previous studies suggesting that there is a need of supplying an additional
135 nitrogen source to promote n-damo bacteria growth, as they are unable to extract it from their
136 denitrification pathway (Wang et al., 2019). Macronutrients and trace compounds used in the
137 enrichment were the proposed by Allegue et al. (2018), and the same feeding strategy was
138 performed. Aluminum foil feeding bags, which are totally impermeable to oxygen, were used
139 and feeding was deoxygenated to avoid the presence of oxygen by using nitrogen gas during
140 10 min. A programmable PLC Micro 820 (Allen-Bradley) connected to a computer was used
141 to control the operation of the system. Apart from the liquid feed, 9 L d⁻¹ of a gas mixture,
142 composed of 95% of CH₄ and 5% of CO₂, were supplied to the system by using a mass-flow
143 controller 4800 Series (Brooks). CO₂ provided buffer capacity to the system as well as the
144 sodium bicarbonate added in the liquid feed. A 5.5 L min⁻¹ recirculation gas from the top of
145 the reactor to the bottom using a mini laboratory blower N 86 KT. 18 (Laboport) made
146 available methane and CO₂ in excess in order to avoid electron donor or buffer limitation,
147 attain complete mixing and prevent membrane fouling.

148 Twelve OMPs known to be present in sewage, were spiked continuously to the synthetic
149 feed: three neurodrugs (fluoxetine FLX, carbamazepine CBZ, diazepam DZP), four
150 antibiotics (erythromycin ERY, roxithromycin ROX, sulfamethoxazole SMX, trimethoprim
151 TMP), three endocrine disruptors (estrone E1, β -estradiol E2, 17 α -ethinylestradiol EE2), and
152 two anti-inflammatories (ibuprofen IBP and naproxen NPX). They were spiked on day 35 at
153 a concentration of 1 ppb, to simulate environmental concentrations. Sampling was limited to

154 the liquid phase (feed and permeate), because of the low biomass concentration inside the
155 reactor and the limited affinity of the selected OMPs to sorb onto solids.

156 **2.2 Analytical methods**

157 Temperature, pH, nitrogen species, total suspended solids (TSS), volatile suspended solids
158 (VSS) and dissolved organic carbon (DOC) were measured according to Standard Methods
159 (Rice et al., 2012). The dissolved oxygen (DO) concentration in the feeding bags was
160 recorded by using a multi-parameter meter (Hach HQ40d) connected to a luminescent optical
161 probe (IntelliCAL LDO101). Gas flow was measured by using a Milli GasCounter MGC-1
162 V3.3 PMMA (Ritter) and its composition was measured in a gas chromatograph (HP 5890
163 Series II) with a Porapack Q 80/100 2 m × 1.8” (SUPELCO) column.

164 Microbial community was characterized by withdrawing a homogeneous biomass sample
165 from the reactor, fixing in 4% v/v paraformaldehyde for fluorescence *in situ* hybridization
166 (FISH) and keeping biomass samples frozen for DNA extraction. FISH was performed as
167 described by Regueiro et al. (2012), with specific probes for n-damo bacteria, damo archaea
168 and anammox bacteria. Sequencing of the 16s rRNA gene was carried out according to the
169 protocol described by Allegue et al. (2018). Raw sequences processing was carried out with
170 USEARCH v11.1. Clustering into Operational Taxonomic Units (OTUs) was performed with
171 the UPARSE algorithm taking into account a 97% of sequence similarity.

172 OMPs analysis samples were collected in amber glass bottles, prefiltered (AP3004705,
173 Millipore), stored at 4 °C and pre-concentrated by using solid phase extraction (SPE) in 3 mL
174 OASIS HLB cartridges. Pre-concentrated samples were analyzed by LC-MS-MS for
175 antibiotics, hormones and neurodrugs, while anti-inflammatories were analyzed by GC-MS.

176 Analytical procedure, equipment, quantification limits and recoveries were described by
177 Alvarino et al. (2015).

178 **3. RESULTS AND DISCUSSION**

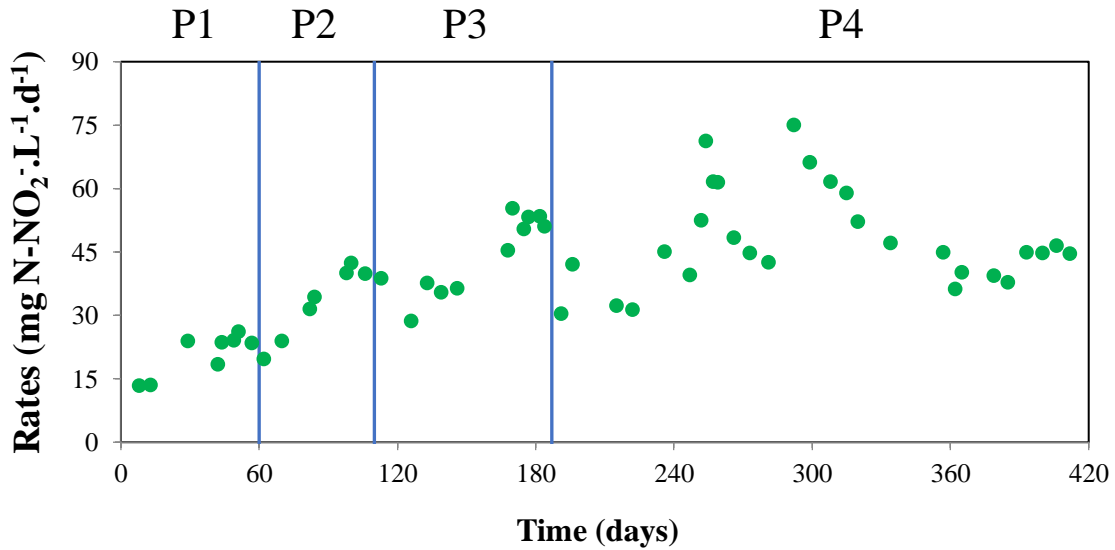
179 ***3.1 MBR performance***

180 The n-damo MBR has been operated for 412 days at 28.3 ± 0.5 °C, with a hydraulic retention
181 time (HRT) of 23.76 ± 0.96 h. The nitrite loading rate (NLR) was increased according to the
182 nitrite removal rates achieved (NRR), maintaining always a low value of residual nitrite in
183 the system to control the MBR activity. Four different periods can be observed, according to
184 activity increase and OMPs sampling campaigns (Fig. 1).

185 Period 1 (days 0-57) corresponded to the start-up of the reactor. A significant NRR of 13.4
186 $\text{mg N L}^{-1} \text{d}^{-1}$ was achieved after 8 d of operation which was progressively increased to 24 mg
187 $\text{N L}^{-1} \text{d}^{-1}$ until the day 29. NRR was maintained in 24.3 ± 1.3 $\text{mg N L}^{-1} \text{d}^{-1}$ from day 44 to 57,
188 during the OMPs sampling campaign. Depletion of oxygen and using impermeable-to-
189 oxygen feeding bags, as indicated Allegue et al. (2018), led to a faster start-up regarding
190 other studies (Bhattacharjee et al., 2016; Ma et al., 2017). In Period 2 (days 58-106) NRR
191 was increased and maintained at 40.8 ± 1.4 $\text{mg N L}^{-1} \text{d}^{-1}$ from day 98 to day 106. The same
192 strategy was followed in Period 3 (days 107-184), where activity was increased up to $52.6 \pm$
193 1.3 $\text{mg N L}^{-1} \text{d}^{-1}$ from day 177 to day 184. Other studies reported similar removal rates using
194 a membrane bioreactor for n-damo enrichment like Kampman et al. (2014) who achieved 36-
195 40 $\text{mg N-NO}_2^- \text{L}^{-1} \text{d}^{-1}$ or in sequence batch reactors like Hu et al. (2019) who achieved a
196 maximum rate of 58.61 $\text{mg N L}^{-1} \text{d}^{-1}$.

197 Period 4 (days 185-412) was characterized by reactor instability which appears to be quite
198 frequent in these systems, when applying higher nitrite loading rates (Kampman et al., 2014).
199 Besides, in the beginning of period 4 there was a decrease in the reactor activity (from 52.6
200 to 31-32 mg N L⁻¹ d⁻¹) due to technical problems with the blower and the seal of the MBR.
201 This implied that some air entered the reactor, severely affecting the n-damo performance,
202 which is extremely sensitive to oxygen exposure (Luesken et al., 2012). We suggest that part
203 of the nitrogen removal rate during this unstable period of operation could be attributed to
204 conventional heterotrophic denitrifiers present in the reactor biomass, that could use the
205 decay n-damo biomass products to denitrify the NO₂ in the reactor, as previously reported in
206 Allegue et al. (2018). This resulted in the increase of NRR with maximum values achieved
207 between days 250 and 320 (Fig. 1). After solving the problem, denitrification activity became
208 stable at the end of Period 4 at a NRR of 39.1 ± 1.2 mg N L⁻¹ d⁻¹, similar to that of Period 2.

209 In Periods 1, 2 and 3 no biomass growth was observed, being the measured TSS and VSS
210 concentration around 0.53 g TSS L⁻¹ and 0.41 g VSS L⁻¹, respectively. This was expected
211 according to the very low growth rates of this type of microorganisms, whose doubling time
212 was estimated in 11.5 days (Allegue et al., 2018). However, an important fraction of the
213 biomass was observed to be attached to the reactor walls, which made the accurate
214 quantification of solids complicated, as reported in previous studies (Kampman et al., 2014).
215 At the beginning of period 4, biomass concentration decreased to concentrations about 0.25
216 g TSS L⁻¹ and 0.21 g VSS L⁻¹, probably due to biomass decay, which was then kept constant
217 from day 357 onwards.



218

219 **Figure 1.** Volumetric nitrite consumption rate according to the different periods.

220 OMPs sampling campaigns were made at the end of each of the four operating periods when

221 stable conditions were maintained, with a specific nitrite removal rates of 54.6 ± 4.9 , $94.8 \pm$

222 3.2 , 131.5 ± 3.3 and 186.3 ± 5.5 mg N g VSS⁻¹ d⁻¹ and a pH of 6.8, 7.2, 7.5 and 7.4, in Period

223 1, 2, 3 and 4, respectively.

224 The ammonia fed to the culture during the whole operation was low in order to prevent the

225 proliferation of anammox bacteria. Ammonia consumption was lower than 1 mg N L⁻¹ d⁻¹ in

226 the first 146 days. After this period, ammonia consumption varied between 2 and 4 mg N L⁻¹

227 d⁻¹. However, the ammonia addition in this study did not cause any observable effect on the

228 development of the n-damo community.

229 **3.2 Microbial community dynamics**

230 Once a significant n-damo activity was achieved in the system (NRR of 13.4 mg N L⁻¹ d⁻¹

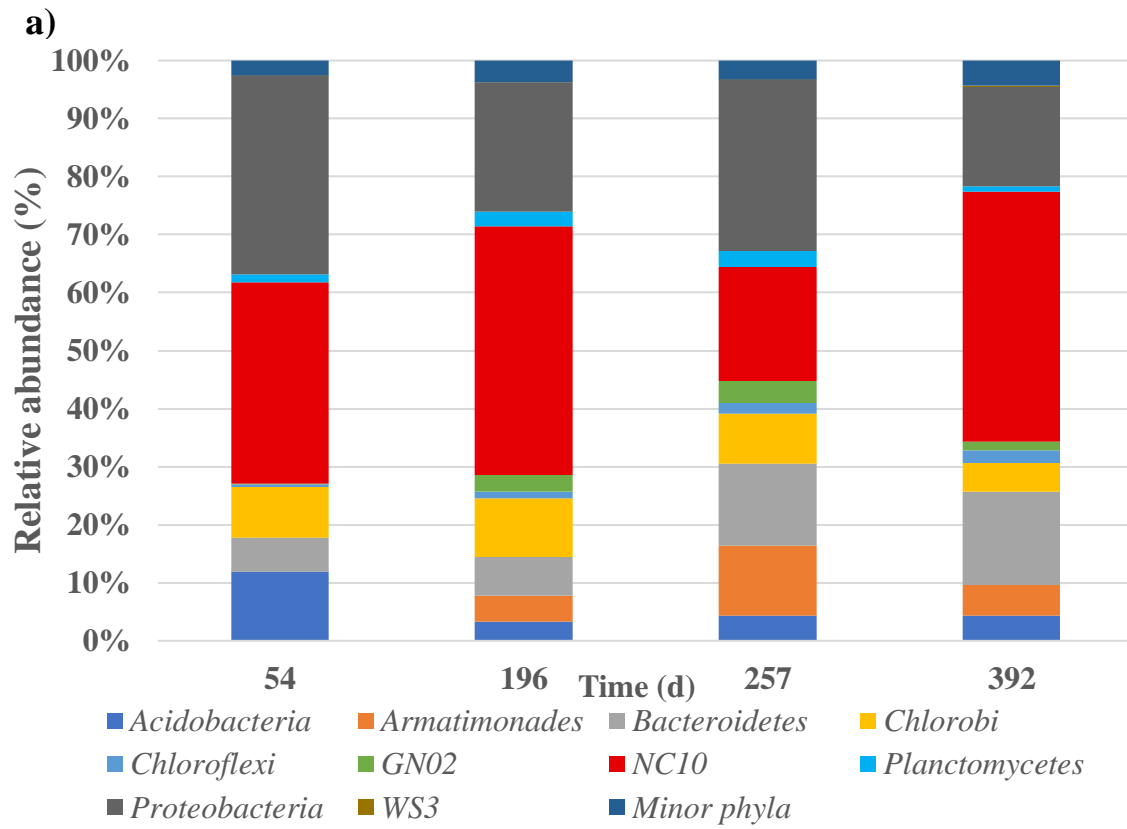
231 were achieved after 8 days of operation), the microbial community dynamics were monitored

232 by FISH and 16s RNA gene sequencing. FISH probes were used on days 29 and 54 of P1

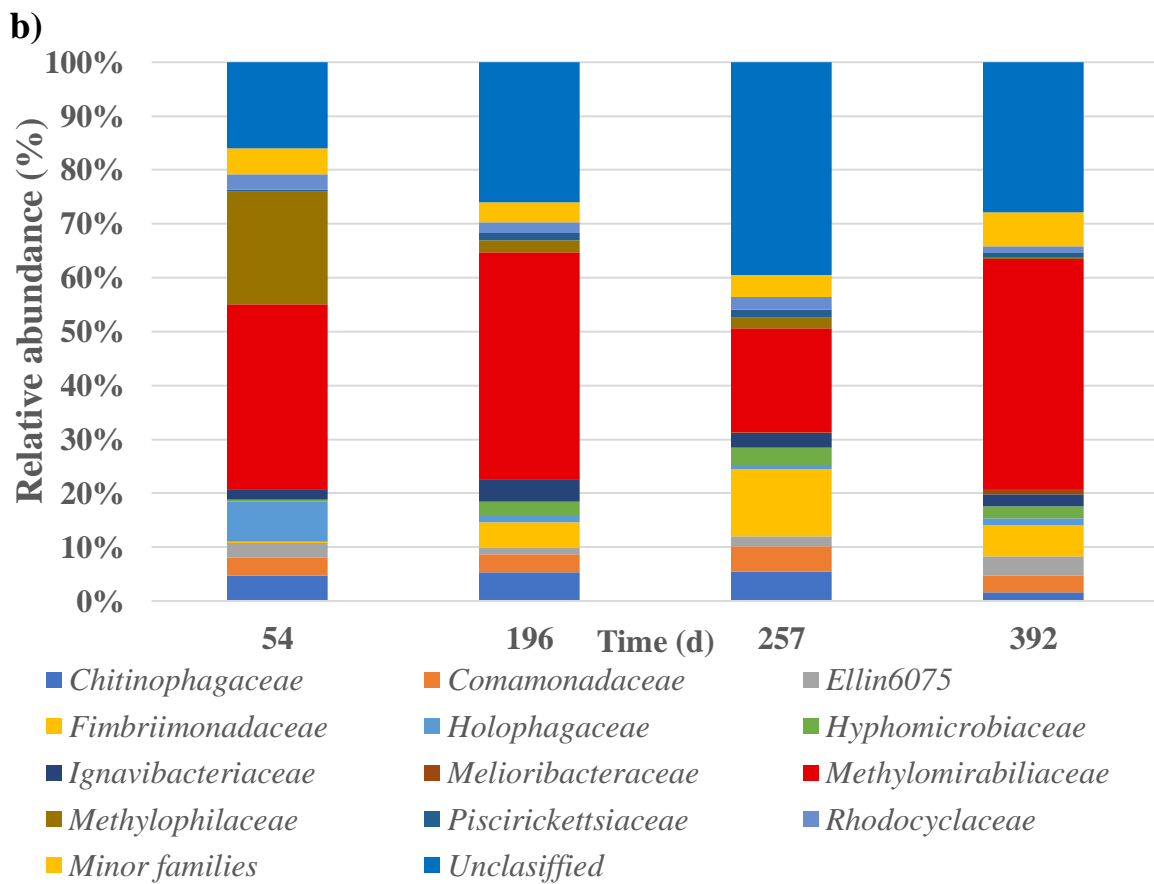
233 and 196 of P3 to check the presence of n-damo bacteria, n-damo archaea and anammox. On
234 day 29, n-damo bacteria were detected (Fig. S2), confirming the fast start-up of the MBR.
235 The culture enrichment was further confirmed by the increasing abundance of n-damo
236 bacteria observed from day 54 onwards. Besides, FISH analyses confirmed the absence of n-
237 damo archaea and anammox expected from the nitrogen mass balances.

238 In addition to FISH analysis, 16s RNA gene sequences were analyzed at four different days
239 of the MBR operation, in order to have a complete information of the microbial composition:
240 days 54 (end of P1), 196 (end of P3), 257 and 392 (unstable and stable operation in P4,
241 respectively). Additionally, quantitative information on the n-damo bacteria enrichment was
242 sought. Table S1 shows the number of bacterial sequences read and the bacterial taxonomic
243 units (OTUs) and singletons identified in each sample. The taxonomic allocation varied from
244 81.70% when classifying OTUs at phyla level to 32.63% at family level. Archaea
245 microorganisms were not analyzed by this method, due to its absence in the FISH analyses.

246 OTUs were distributed among 37 different phyla in which the most abundant ones (>1%)
247 represent the $96.6\% \pm 0.74\%$ of total OTUs distributed in this taxonomic level (Fig. 2). The
248 NC10 phylum, the one associated with n-damo bacteria (Ettwig et al., 2010), was the
249 predominant in 3 samples followed by the *Proteobacteria* phylum. In the third sample, due
250 to the operational problems and the entrance of air in the system mentioned in the section
251 3.1., the relative abundance of NC10 phylum decreased sharply (from around 40% to 20%).
252 As it is mentioned in other studies, n-damo bacteria is very sensitive to oxygen (Luesken et
253 al., 2012), so this may be the reason for the decrease in the n-damo abundance. Thus, being
254 in contact with air not only affected the MBR performance in terms of nitrogen removal, but
255 also modified the microbial composition.



256



257

258 **Figure 2.** Microbial communities present in MBR through the whole operation. a) Bacteria
259 phyla and b) Bacteria families with relative abundances over 1%.

260

261 Species were distributed in more than 100 families in which *Methylomirabiliaceae*, the
262 family of *Candidatus Methylomirabilis oxyfera* associated with the NC10 phylum, was the
263 most abundant one in all samples. A significant relative abundance (around 20%) was
264 detected in the first sample of *Methylophylaceae* family, a known methylophile, probably
265 coming from the inoculum. However, their presence in the MBR is reduced in the next
266 samples, being his relative abundance in the last point around 0.26%. As in other studies (Fu
267 et al., 2017; Wang et al., 2019), there was a presence of other conventional denitrifying
268 heterotrophs, like *Comamonaceae* and *Hyphomicrobiaceae*. Their relative abundance was
269 higher at day 257, 4.73% and 3.26% respectively, in which the mixing liquor was exposed
270 to air. As it was mentioned in the previous section, they probably use biomass decay products
271 to perform the conventional denitrification (Allegue et al., 2018). Nevertheless, these
272 bacterial families never constituted the major groups in the MBR community (less than 4%
273 in both cases). What is clear from the 16s RNA gene sequences analysis is the negative
274 impact of the oxygen entrance to the reactor on n-damo bacteria enrichment, stating as crucial
275 the maintenance of an anoxic environment in the system.

276 Due to the oxygen depletion in the feeding bags, the presence of aerobic methanotrophs, like
277 the family *Methylococcaceae*, only represented the 0.15% in the first sample and less than
278 0.02% in the rest of them. In the same line, *Brocadiaceae* family only represented the 0.06
279 % of the total microbial community, indicating that despite the addition of a low quantity of
280 ammonium in the feeding bags, the presence of anammox bacteria in the whole culture was
281 negligible, since the species belonging to this family (*Candidatus Brocadia*) are one of the

282 most common organisms found in the enrichments of wastewater treatment technologies
283 (Kuenen, 2008). Although Luesken et al. (2011) proposed that anammox bacteria have higher
284 affinity for NO_2^- than n-damo bacteria, its minor presence in the whole culture of the reactor
285 suggests a residual contribution to denitrification .

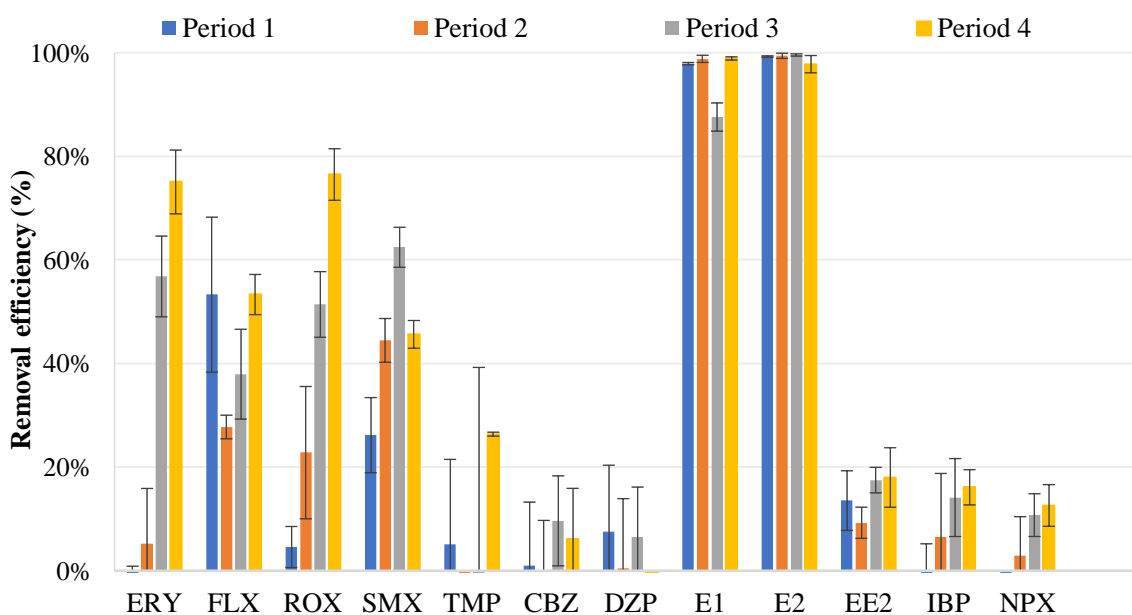
286 According to the FISH analyses, the operational results in terms of nitrogen removal and the
287 16s RNA gene sequence (Illumina), an enrichment of the culture in n-damo bacteria was
288 clearly achieved. The relative abundance values of the NC10 phylum were similar that those
289 reported in Allegue et al. (2018), in a very similar enrichment procedure and system. Due to
290 the low abundance of other denitrifying groups, like anammox or heterotrophic denitrifying
291 bacteria, it is assumed that n-damo bacteria is responsible for almost all the nitrogen removed
292 in the MBR.

293 All the changes in the bacterial community occurred when the MBR performance suffered
294 operational issues; there was no evidence that the presence of the OMPs affected the
295 microbial community.

296 ***3.3 OMPs results***

297 The OMPs removal efficiency was studied in the system at the end of each operational period
298 (Section 3.1) to determine their removal efficiency for the different specific activities
299 achieved in the reactor (Fig. 3) and maintained stable at least for 10-15 days. Sorption was
300 not considered as a relevant removal mechanism in this study because the studied OMPs are
301 not lipophilic, except for FLX (whose particular behavior is discussed in section 3.4).
302 Additionally, the concentration of VSS during the MBR performance was very low ($< 0.4 \text{ g}$
303 $\text{VSS}\cdot\text{L}^{-1}$) supporting the statement of low contribution of sorption to OMP removal.

304 According to the reported values of the Henry coefficients for the selected OMPs, neither
 305 volatilization supposed a relevant removal mechanism (Suárez et al., 2008). Consequently,
 306 the OMP removal efficiencies determined in this work were attributed to biotransformation.
 307 Accordingly, the selected OMPs can be grouped in the following three categories: recalcitrant
 308 compounds (removal efficiency < 20%) such as TMP, CBZ, DZP, EE2, IBP, NPX and DCF;
 309 highly biotransformable substances (> 90%) including E1 and E2; and compounds
 310 moderately biotransformed in the reactor (20-80%) as ERY, SMX, ROX and FLX.



311

Figure 3. Removal efficiencies of the selected OMPs in each stage.

312

313 As expected, the removal efficiency of CBZ and DZP barely reached 10% in any of the 4
 314 sampling campaigns. Their recalcitrant behavior in the three redox environments was
 315 previously pointed out in several studies (Alvarino et al., 2018; Suarez et al., 2010).
 316 Regarding IBP, its biotransformation degree was around 15% in the last two stages. In this
 317 work, IBP proved to be much more recalcitrant in anoxic environments compared to removal
 318 efficiencies reported in aerobic reactors, with conventional heterotrophic bacteria

319 (Fernandez-Fontaina et al., 2016). However, this low biotransformation degree in anoxic
320 conditions is in accordance with by previous batch experiments using a synthetic media with
321 acetate and nitrate (Kassotaki et al., 2018) or fed with pre-clarified wastewater with an
322 external nitrate addition (Torresi et al., 2017). Thus, we can confirm that IBP biodegradation
323 is highly influenced by redox conditions. According to Falås et al. (2013), the removal of this
324 compound is strongly influenced by the physical conformation of the biomass, achieving
325 better results with biomass attached to carriers than suspended in the mixed liquor.

326 The high removal of natural hormones as well as the recalcitrant behavior of the EE2, was
327 observed previously in a denitrifying activated sludge reactor (Suarez et al., 2010).
328 Nevertheless, the removal efficiencies obtained in this study for natural hormones are higher
329 (almost 100% of biodegradation versus 72%) than those reported by Suarez et al. (2010). No
330 effect was observed in the removal of natural and synthetic hormones during the reactor
331 operation. Despite having a similar chemical structure, a steric impediment was suggested in
332 other studies to explain the different removal efficiencies achieved for the hormones E2 and
333 EE2 (Czajka and Londry, 2006).

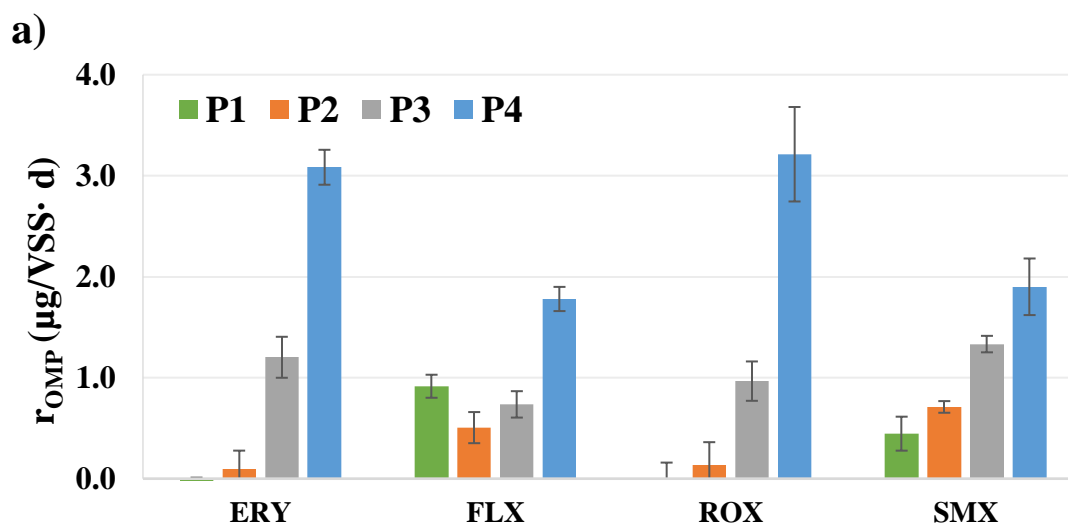
334 In the case of the moderately biodegradable compounds (ERY, ROX, SMX and FLX) the
335 removal efficiency observed during the reactor operation varied strongly (< 10% up to >
336 70%). This behavior will be further discussed in section 3.4. In the anoxic chamber of a pilot
337 plant which combined the three redox conditions, Arias et al., (2018) found a 30% removal
338 efficiency for ROX and ERY, comparable with the removal found in the aerobic
339 compartment. Moreover, Burke et al. (2014) observed a preferential biodegradation of ROX
340 under anoxic compared to aerobic conditions. In the case of SMX, its removal is commonly
341 associated with anaerobic conditions (Alvarino et al., 2018; Arias et al., 2018). Nevertheless,

342 significant biotransformation rates were reported in anoxic denitrifying conditions in batch
343 tests, in agreement with the results obtained in this research (Kassotaki et al., 2018; Polese
344 et al., 2017; Torresi et al., 2017). According to Torresi et al. (2017), when the primary
345 substrate of the microbial consortia is available, the removal rate of SMX is enhanced,
346 suggesting that the main biotransformation mechanism of this compound is cometabolism.
347 Concerning FLX, some authors suggested that its removal is mainly attributed to sorption in
348 anoxic environments (Alvarino et al., 2018; Pomiès et al., 2015). This could explain the high
349 removal efficiency observed for FLX already in P1 (Fig. 3) as further discussed in the next
350 section. On the other hand, Suarez et al. (2010) reported a high removal of FLX in an anoxic
351 denitrifying reactor with a strong influence of the SRT on its biodegradation. Thus, the
352 removal of this compound could be enhanced with time in the reactor as no purges of biomass
353 were carried out throughout its operation.

354 ***3.4 Cometabolic biotransformation of antibiotics***

355 The behavior of FLX, ROX, ERY and SMX could suggest removal by cometabolism,
356 according to the increasing trend in their removal efficiencies along the different operational
357 periods. Since the OMPs concentration fed to the bioreactor was the same during the whole
358 operation, if the biodegradation rate of one compound increased in parallel to the n-damo
359 primary metabolism we suggest that this pollutant was cometabolically biotransformed. In
360 order to analyze this, the specific removal rates of the primary substrate (nitrite) and the
361 OMPs were plotted in Fig 4. For this purpose, the data from the OMP concentrations in the
362 feed and in the permeate, the applied HRT and the measured VSS concentration in the reactor
363 were considered for each period of operation. The denitrifying specific activity in each stage
364 was specified in the section 3.1.

365



366

b)

	Line equation	R ²
ERY	y: 0.0344x - 3.3274	0.9999
FLX	y: 0.0152x - 1.1011	0.9598
ROX	y: 0.0361x - 3.5831	0.9885
SMX	y: 0.0133x - 0.5420	0.9686

367

368 **Figure 4.** (a) Specific micropollutant removal rate for ERY, FLX, ROX and SMX at
 369 different specific biomass activity. (b) Linear regression equation and correlation
 370 coefficient (R²) for each compound (y is the specific removal rate of each compound and x
 371 is the specific removal rate for nitrite) and considering the data for periods P2-P4.

372

373 The linear correlations in Fig. 4b showed a clear relationship between the or specific primary
 374 substrate removal rate and the specific removal rate of ERY, SMX, ROX and FLX between
 375 P2 and P4. This implies that best results in terms of OMPs biotransformation kinetics were
 376 achieved in P4, when the specific denitrification capacity of the n-damo bacteria was the
 377 highest. Even in the case of SMX, for which a lower removal efficiency (45.6%) was
 378 measured in P4 (Fig. 3), the specific removal rate in this period was higher than in the

379 previous operational periods, supporting cometabolic features. Between the first and the
380 second sampling campaign, there were no significant differences in the specific removal rate
381 of the OMPs, with the exception of FLX. If cometabolism is the main biodegradation
382 mechanism, some authors suggest that enough growth substrates are necessary to stimulate
383 the creation of the relevant enzymes for the degradation of the OMPs (Tran et al., 2013). This
384 may have occurred in the first sampling period (P1), when the nitrite concentration fed to the
385 system was the lowest of the total reactor operation ($20 \text{ mg N L}^{-1} \text{ d}^{-1}$ of NRL). So, for that
386 reason the results obtained in the period 1 were not included when considering the
387 cometabolic data analysis (Fig. 4).

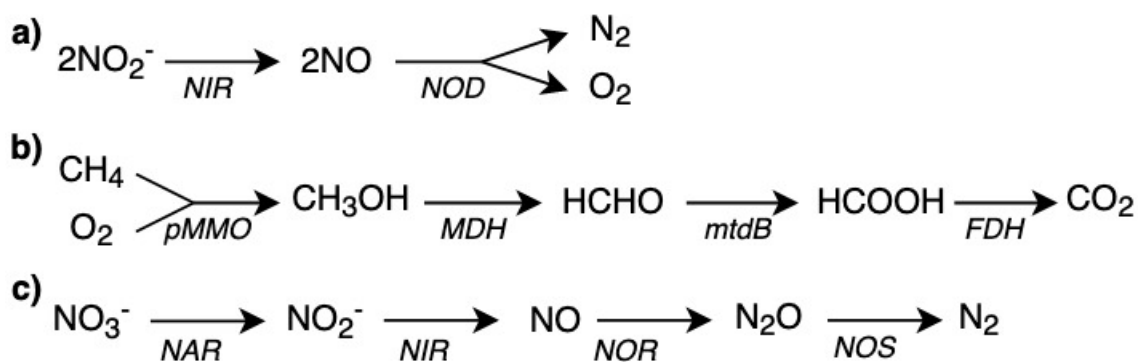
388 In the case of FLX, the higher specific removal rate achieved in P1 compared to the other
389 OMPs may be due to its sorption onto the sludge in the MBR. Considering a K_d of 1000 L
390 kgTSS^{-1} (Alvarino et al., 2016) for this compound, the removal would be almost completely
391 associated to such mechanism (concentration in feed: 1 ppb , 0.51 gTSS L^{-1} in P1) since its
392 global removal efficiency was around 50% (Fig. 3). The sorption coefficient of this
393 compound may be slightly higher in anoxic environments, however the order of magnitude
394 is the same and sorption is more dependent on the physico-chemical characteristics of the
395 micropollutants and the biomass conformation than to redox environment (Alvarino et al.,
396 2018). Pomiès et al. (2015) exposed that FLX removal in anoxic conditions was mainly due
397 to sorption, with little influence of biodegradation. However, once sorption equilibrium is
398 established, normally after several days of contact between the sludge and the OMPs,
399 biotransformation becomes the main removal mechanism (Yang et al., 2011). Thus, from P1
400 onwards, the removal of FLX could be attributed fully to biodegradation, due to the

401 negligible biomass growth during the whole reactor operation and only values from P2 to P4
402 have been considering for the correlation with the specific nitrite removal of the reactor.

403 In previous studies, the removal of SMX has been associated with the activity of aerobic
404 autotrophic and heterotrophic bacteria. Its biotransformation rate was positively correlated
405 with the presence of organic matter as main substrate (Alvarino et al., 2018; Fernandez-
406 Fontaina et al., 2016). However, in our study no correlation has been found between the
407 presence of the primary substrate (nitrite) with the microcontaminants removal rate. Polesel
408 et al. (2017) reported a clear correlation between the specific denitrification rate and the
409 biotransformation constant of SMX and ERY (the correlation coefficient reported is greater
410 than 0.95) in batch assays with heterotrophic denitrification bacteria, in agreement with our
411 results. Their denitrification range varied between 10 and 50 mg N gTSS⁻¹ d⁻¹, consequently
412 focusing on lower levels than the present research (50-190 mg N gVSS⁻¹ d⁻¹). In Fig. 4b)
413 different slopes were determined for the OMP studied, showing that ERY and ROX were
414 more influenced by the cometabolic effect than SMX and FLX. This may indicate that
415 cometabolism is more dependent to the specific denitrification rates, as it was previously
416 reported (Polesel et al., 2017; Torresi et al., 2018), than to the presence of high concentration
417 of the primary substrate as in P2 and P4 the NRR was almost the same (around 40 mg N L⁻¹
418 d⁻¹) but the specific nitrite removal rate in such periods was different.

419 It is worth to note that most results on OMP removal under anoxic conditions have been
420 published for conventional denitrification processes. Since the nitrogen removal metabolism
421 of the n-damo process is different from conventional denitrification (Fig. 5c), the behavior
422 of OMP in those processes could be different. In conventional denitrification, the nitrate is
423 progressively reduced to nitrite, nitric oxide, nitrous oxide and, finally, to nitrogen gas.

424 Specially the nitrite reduction pathway is different, due to the presence of and NO dismutase
 425 (NOD) which performs the last step of the denitrification and provides O₂ for the methane
 426 oxidation (Fig. 5a) (Wu et al., 2011). The common enzyme between both processes, the
 427 copper nitrite reductase (EC 1.7.2.1) (NIR), was correlated with the biotransformation rate
 428 constant of some compounds like SMX, ERY or TMP and the abundance of the gene
 429 encoding for these enzyme (Torresi et al., 2018). However, there are other enzymes in the
 430 methane oxidation pathway like monooxygenases (particulate methane monooxygenase
 431 (*pMMO*) (EC 1.14.18.3)) or dehydrogenases (methanol dehydrogenase (MDH) (EC 1.1.2.7))
 432 which can be other candidates to biotransform OMPs, as they are known to participate in
 433 some pollutant degradations such as toluene or xylene (Jindrová et al., 2002). Further
 434 research needs to be done to elucidate which enzymes in the n-damo metabolism are
 435 responsible for these biotransformations.



437 **Figure 5.** Candidatus *M. oxyfera* metabolic pathways. (a) Nitrite pathway, (b) Methane
 438 pathway. (c) Conventional heterothrophic denitrification chain. Abbreviations: NIR; nitrite
 439 reductase (EC 1.7.2.1); NOD, nitric oxide dismutase; *pMMO*, particulate methane mono-
 440 oxygenase (EC 1.14.18.3); MDH, methanol dehydrogenase (EC 1.1.2.7) ; *mtdB*,
 441 methylene-H4MPT dehydrogenase (EC 1.5.1.5); FDH, fromate dehydrogenase (EC
 442 1.17.1.10); NAR, nitrite reductases (EC 1.7.1.1); NOR, nitric oxide reductase (EC 1.7.5.2);
 443 NOS, nitrous oxide reductase (EC 1.7.2.4).

444
 445

446 4. CONCLUSIONS

447 This research provided new knowledge about the capability of n-damo cultures to
448 biotransform OMPs. A successful n-damo enrichment was achieved along 412 d of operation
449 in a MBR. Limiting the quantity of oxygen entering the MBR, by sealing efficiently the
450 reactor and deoxygenating the feeding bags, was revealed as a crucial factor in order to
451 achieve a fast n-damo bacteria enrichment and denitrification activity ($24 \text{ mg N L}^{-1} \text{ d}^{-1}$ in
452 around 30 days). The system also showed its robustness, being able to recover the previous
453 denitrifying activity ($40 \text{ mg N L}^{-1} \text{ d}^{-1}$), after an inhibitory period. The 16S rRNA gene
454 sequencing results showed that *Methylomirabaliaceae* family dominated the microbial
455 community with a relative abundance of 40 % during stable reactor operation. The OMPs
456 could be classified according to the achieved removal efficiencies in the reactor as:
457 recalcitrant, completely biodegradable and moderately biodegradable. For the moderately
458 biodegradable OMPs (ERY, ROX, SMX and FLX), a positive correlation between the n-
459 damo bacteria denitrification kinetics and the OMP specific biotransformation rates has been
460 found. This suggests that the main mechanism driving such biotransformation was
461 cometabolism.

462 **5. ACKNOWLEDGEMENTS**

463 This research was carried out with the financial support received from Spanish Ministry of
464 Economy and Competitiveness through the project COMETT (CTQ2016-80847-R), co-
465 funded by FEDER. M. Martínez would also like to express his gratitude to the same Ministry
466 for awarding a research scholarship (BES-2017-080503). The authors belong to the Galician
467 Competitive Research Group GRC (ED431C 2017/29), programme co-funded by FEDER,
468 and to CRETUS Strategic Partnership (ED431E 2018/01).

470 **References**

- 471 Allegue, T., Arias, A., Fernandez-Gonzalez, N., Omil, F., Garrido, J.M., 2018. Enrichment
472 of nitrite-dependent anaerobic methane oxidizing bacteria in a membrane bioreactor.
473 Chem. Eng. J. 347, 721–730. <https://doi.org/10.1016/j.cej.2018.04.134>
- 474 Alvarino, T., Suárez, S., Garrido, M., Lema, J.M., Omil, F., 2016. A UASB reactor coupled
475 to a hybrid aerobic MBR as innovative plant configuration to enhance the removal of
476 organic micropollutants. Chemosphere 144, 452–458.
477 <https://doi.org/10.1016/j.chemosphere.2015.09.016>
- 478 Alvarino, T., Suarez, S., Katsou, E., Vazquez-Padin, J., Lema, J.M., Omil, F., 2015.
479 Removal of PPCPs from the sludge supernatant in a one stage nitrification/anammox
480 process. Water Res. 68, 701–709. <https://doi.org/10.1016/j.watres.2014.10.055>
- 481 Alvarino, T., Suarez, S., Lema, J., Omil, F., 2018. Understanding the sorption and
482 biotransformation of organic micropollutants in innovative biological wastewater
483 treatment technologies. Sci. Total Environ. 615, 297–306.
484 <https://doi.org/10.1016/j.scitotenv.2017.09.278>
- 485 Arias, A., Alvarino, T., Allegue, T., Suárez, S., Garrido, J.M., Omil, F., 2018. An
486 innovative wastewater treatment technology based on UASB and IFAS for cost-
487 efficient macro and micropollutant removal. J. Hazard. Mater. 359, 113–120.
488 <https://doi.org/10.1016/j.jhazmat.2018.07.042>
- 489 Bhattacharjee, A.S., Motlagh, A.M., Jetten, M.S.M., Goel, R., 2016. Methane dependent
490 denitrification- from ecosystem to laboratory-scale enrichment for engineering
491 applications. Water Res. 99, 244–252. <https://doi.org/10.1016/j.watres.2016.04.070>

492 Burke, V., Richter, D., Hass, U., Duennbier, U., Greskowiak, J., Massmann, G., 2014.
493 Redox-dependent removal of 27 organic trace pollutants: Compilation of results from
494 tank aeration experiments. *Environ. Earth Sci.* 71, 3685–3695.
495 <https://doi.org/10.1007/s12665-013-2762-8>

496 Czajka, C.P., Londry, K.L., 2006. Anaerobic biotransformation of estrogens. *Sci. Total*
497 *Environ.* 367, 932–941. <https://doi.org/10.1016/j.scitotenv.2006.01.021>

498 Ettwig, K.F., Butler, M.K., Le Paslier, D., Pelletier, E., Mangenot, S., Kuypers, M.M.M.,
499 Schreiber, F., Dutilh, B.E., Zedelius, J., De Beer, D., Gloerich, J., Wessels, H.J.C.T.,
500 Van Alen, T., Luesken, F., Wu, M.L., Van De Pas-Schoonen, K.T., Op Den Camp,
501 H.J.M., Janssen-Megens, E.M., Francoijs, K.J., Stunnenberg, H., Weissenbach, J.,
502 Jetten, M.S.M., Strous, M., 2010. Nitrite-driven anaerobic methane oxidation by
503 oxygenic bacteria. *Nature* 464, 543–548. <https://doi.org/10.1038/nature08883>

504 Ettwig, K.F., Van Alen, T., Van De Pas-Schoonen, K.T., Jetten, M.S.M., Strous, M., 2009.
505 Enrichment and molecular detection of denitrifying methanotrophic bacteria of the
506 NC10 phylum. *Appl. Environ. Microbiol.* 75, 3656–3662.
507 <https://doi.org/10.1128/AEM.00067-09>

508 Falås, P., Longrée, P., La Cour Jansen, J., Siegrist, H., Hollender, J., Joss, A., 2013.
509 Micropollutant removal by attached and suspended growth in a hybrid biofilm-
510 activated sludge process. *Water Res.* 47, 4498–4506.
511 <https://doi.org/10.1016/j.watres.2013.05.010>

512 Fernandez-Fontaina, E., Gomes, I.B., Aga, D.S., Omil, F., Lema, J.M., Carballa, M., 2016.
513 Biotransformation of pharmaceuticals under nitrification, nitrataion and heterotrophic
514 conditions. *Sci. Total Environ.* 541, 1439–1447.
515 <https://doi.org/10.1016/j.scitotenv.2015.10.010>

516 Fischer, K., Majewsky, M., 2014. Cometabolic degradation of organic wastewater
517 micropollutants by activated sludge and sludge-inherent microorganisms. *Appl.*
518 *Microbiol. Biotechnol.* 98, 6583–6597. <https://doi.org/10.1007/s00253-014-5826-0>

519 Fu, L., Ding, J., Lu, Y., Ding, Z., Zeng, R.J., 2017. Nitrogen source effects on the
520 denitrifying anaerobic methane oxidation culture and anaerobic ammonium oxidation
521 bacteria enrichment process. *Appl. Microbiol. Biotechnol.* 101, 3895–3906.
522 <https://doi.org/10.1007/s00253-017-8163-2>

523 Gonzalez-Gil, L., Krah, D., Ghattas, A.K., Carballa, M., Wick, A., Helmholz, L., Lema,
524 J.M., Ternes, T.A., 2019. Biotransformation of organic micropollutants by anaerobic
525 sludge enzymes. *Water Res.* 152, 202–214.
526 <https://doi.org/10.1016/j.watres.2018.12.064>

527 He, Z., Cai, C., Wang, J., Xu, X., Zheng, P., Jetten, M.S.M., Hu, B., 2016. A novel
528 denitrifying methanotroph of the NC10 phylum and its microcolony. *Sci. Rep.* 6, 1–
529 10. <https://doi.org/10.1038/srep32241>

530 Hu, Z., Ru, D., Wang, Y., Zhang, J., Jiang, L., Xu, X., Nie, L., 2019. Optimization of a
531 nitrite-dependent anaerobic methane oxidation (n-damo) process by enhancing
532 methane availability. *Bioresour. Technol.* 275, 101–108.
533 <https://doi.org/10.1016/j.biortech.2018.12.035>

534 Jindrová, E., Chocová, M., Demnerová, K., Brenner, V., 2002. Bacterial Aerobic
535 Degradation of Benzene, Toluene, Ethylbenzene and Xylene. *Folia Microbiol. (Praha).*
536 47, 83–93. <https://doi.org/10.1007/BF02817664>

537 Kampman, C., Temmink, H., Hendrickx, T.L.G., Zeeman, G., Buisman, C.J.N., 2014.
538 Enrichment of denitrifying methanotrophic bacteria from municipal wastewater sludge
539 in a membrane bioreactor at 20°C. *J. Hazard. Mater.* 274, 428–435.

540 <https://doi.org/10.1016/j.jhazmat.2014.04.031>

541 Kassotaki, E., Pijuan, M., Joss, A., Borrego, C.M., Rodriguez-Roda, I., Buttiglieri, G.,
542 2018. Unraveling the potential of a combined nitrification-anammox biomass towards
543 the biodegradation of pharmaceutically active compounds. *Sci. Total Environ.* 624,
544 722–731. <https://doi.org/10.1016/j.scitotenv.2017.12.116>

545 Kuenen, J.G., 2008. Anammox bacteria from discovery. *Nature* 6, 320–326.
546 <https://doi.org/10.1038/nrmicro1857>

547 Liu, T., Hu, S., Guo, J., 2019. Enhancing mainstream nitrogen removal by employing
548 nitrate/nitrite-dependent anaerobic methane oxidation processes. *Crit. Rev.*
549 *Biotechnol.* 39, 732–745. <https://doi.org/10.1080/07388551.2019.1598333>

550 Luesken, F.A., Sánchez, J., van Alen, T.A., Sanabria, J., Op den Camp, H.J.M., Jetten,
551 M.S.M., Kartal, B., 2011. Simultaneous nitrite-dependent anaerobic methane and
552 ammonium oxidation processes. *Appl. Environ. Microbiol.* 77, 6802–6807.
553 <https://doi.org/10.1128/AEM.05539-11>

554 Luesken, F.A., Wu, M.L., Op den Camp, H.J.M., Keltjens, J.T., Stunnenberg, H., Francoijs,
555 K.J., Strous, M., Jetten, M.S.M., 2012. Effect of oxygen on the anaerobic
556 methanotroph “*Candidatus Methyloirabilis oxyfera*”: Kinetic and transcriptional
557 analysis. *Environ. Microbiol.* 14, 1024–1034. [https://doi.org/10.1111/j.1462-](https://doi.org/10.1111/j.1462-2920.2011.02682.x)
558 [2920.2011.02682.x](https://doi.org/10.1111/j.1462-2920.2011.02682.x)

559 Ma, R., Hu, Z., Zhang, J., Ma, H., Jiang, L., Ru, D., 2017. Reduction of greenhouse gases
560 emissions during anoxic wastewater treatment by strengthening nitrite-dependent
561 anaerobic methane oxidation process. *Bioresour. Technol.* 235, 211–218.
562 <https://doi.org/10.1016/j.biortech.2017.03.094>

563 Noyola, A., Morgan-Sagastume, J.M., López-Hernández, J.E., 2006. Treatment of biogas

564 produced in anaerobic reactors for domestic wastewater: Odor control and
565 energy/resource recovery. *Rev. Environ. Sci. Biotechnol.* 5, 93–114.
566 <https://doi.org/10.1007/s11157-005-2754-6>

567 Plosz, B.G., Leknes, H., Thomas, K. V, 2010. Impacts of competitive inhibition, parent
568 compound formation and partitioning behaviour on antibiotic micro-pollutants
569 removal in activated sludge. *Environ. Sci. Technol.* 44, 734–742.

570 Polesel, F., Torresi, E., Loreggian, L., Casas, M.E., Christensson, M., Bester, K., Plósz,
571 B.G., 2017. Removal of pharmaceuticals in pre-denitrifying MBBR – Influence of
572 organic substrate availability in single- and three-stage configurations. *Water Res.*
573 123, 408–419. <https://doi.org/10.1016/j.watres.2017.06.068>

574 Pomiès, M., Choubert, J.M., Wisniewski, C., Miège, C., Budzinski, H., Coquery, M., 2015.
575 Lab-scale experimental strategy for determining micropollutant partition coefficient
576 and biodegradation constants in activated sludge. *Environ. Sci. Pollut. Res.* 22, 4383–
577 4395. <https://doi.org/10.1007/s11356-014-3646-5>

578 Regueiro, L., Veiga, P., Figueroa, M., Alonso-Gutierrez, J., Stams, A.J.M., Lema, J.M.,
579 Carballa, M., 2012. Relationship between microbial activity and microbial community
580 structure in six full-scale anaerobic digesters. *Microbiol. Res.* 167, 581–589.
581 <https://doi.org/10.1016/J.MICRES.2012.06.002>

582 Rice, E.W. (ed), Rice, E.W., Bridgewater, L., Association, A.P.H., Association, A.W.W.,
583 Federation, W.E., 2012. Standard methods for the examination of water and
584 wastewater.

585 Silva-Teira, A., Sánchez, A., Buntner, D., Rodríguez-Hernández, L., Garrido, J.M., 2017.
586 Removal of dissolved methane and nitrogen from anaerobically treated effluents at
587 low temperature by MBR post-treatment. *Chem. Eng. J.* 326, 970–979.

588 <https://doi.org/10.1016/j.cej.2017.06.047>

589 Sousa, J.C.G., Ribeiro, A.R., Barbosa, M.O., Pereira, M.F.R., Silva, A.M.T., 2018. A
590 review on environmental monitoring of water organic pollutants identified by EU
591 guidelines. *J. Hazard. Mater.* 344, 146–162.
592 <https://doi.org/10.1016/j.jhazmat.2017.09.058>

593 Souza, C.L., Chernicharo, C.A.L., Aquino, S.F., 2011. Quantification of dissolved methane
594 in UASB reactors treating domestic wastewater under different operating conditions.
595 *Water Sci. Technol.* 64, 2259–2264. <https://doi.org/10.2166/wst.2011.695>

596 Suárez, S., Carballa, M., Omil, F., Lema, J.M., 2008. How are pharmaceutical and personal
597 care products (PPCPs) removed from urban wastewaters? *Rev. Environ. Sci.*
598 *Biotechnol.* 7, 125–138. <https://doi.org/10.1007/s11157-008-9130-2>

599 Suarez, S., Lema, J.M., Omil, F., 2010. Removal of Pharmaceutical and Personal Care
600 Products (PPCPs) under nitrifying and denitrifying conditions. *Water Res.* 44, 3214–
601 3224. <https://doi.org/10.1016/j.watres.2010.02.040>

602 Torresi, E., Escolà Casas, M., Polesel, F., Plósz, B.G., Christensson, M., Bester, K., 2017.
603 Impact of external carbon dose on the removal of micropollutants using methanol and
604 ethanol in post-denitrifying Moving Bed Biofilm Reactors. *Water Res.* 108, 95–105.
605 <https://doi.org/10.1016/j.watres.2016.10.068>

606 Torresi, E., Gülay, A., Polesel, F., Jensen, M.M., Christensson, M., Smets, B.F., Plósz,
607 B.G., 2018. Reactor staging influences microbial community composition and
608 diversity of denitrifying MBBRs- Implications on pharmaceutical removal. *Water Res.*
609 138, 333–345. <https://doi.org/10.1016/j.watres.2018.03.014>

610 Tran, N.H., Reinhard, M., Gin, K.Y.H., 2018. Occurrence and fate of emerging
611 contaminants in municipal wastewater treatment plants from different geographical

612 regions-a review. *Water Res.* 133, 182–207.
613 <https://doi.org/10.1016/j.watres.2017.12.029>

614 Tran, N.H., Urase, T., Ngo, H.H., Hu, J., Ong, S.L., 2013. Insight into metabolic and
615 cometabolic activities of autotrophic and heterotrophic microorganisms in the
616 biodegradation of emerging trace organic contaminants. *Bioresour. Technol.* 146,
617 721–731. <https://doi.org/10.1016/j.biortech.2013.07.083>

618 Versantvoort, W., Guerrero-Cruz, S., Speth, D.R., Frank, J., Gambelli, L., Cremers, G., van
619 Alen, T., Jetten, M.S.M., Kartal, B., Op den Camp, H.J.M., Reimann, J., 2018.
620 Comparative genomics of *Candidatus Methyloirabilis* species and description of *Ca.*
621 *Methyloirabilis lanthanidiphila*. *Front. Microbiol.* 9, 1–10.
622 <https://doi.org/10.3389/fmicb.2018.01672>

623 Wang, D., Wang, Y., Liu, Y., Ngo, H.H., Lian, Y., Zhao, J., Chen, F., Yang, Q., Zeng, G.,
624 Li, X., 2017. Is denitrifying anaerobic methane oxidation-centered technologies a
625 solution for the sustainable operation of wastewater treatment Plants? *Bioresour.*
626 *Technol.* 234, 456–465. <https://doi.org/10.1016/j.biortech.2017.02.059>

627 Wang, J., Hua, M., Li, Y., Ma, F., Zheng, P., Hu, B., 2019. Achieving high nitrogen
628 removal efficiency by optimizing nitrite-dependent anaerobic methane oxidation
629 process with growth factors. *Water Res.* 161, 35–42.
630 <https://doi.org/10.1016/j.watres.2019.05.101>

631 Wu, M.L., Ettwig, K.F., Jetten, M.S.M., Strous, M., Keltjens, J.T., Van Niftrik, L., 2011. A
632 new intra-aerobic metabolism in the nitrite-dependent anaerobic methane-oxidizing
633 bacterium *Candidatus “Methyloirabilis oxyfera.”* *Biochem. Soc. Trans.* 39, 243–248.
634 <https://doi.org/10.1042/BST0390243>

635 Yang, S.F., Lin, C.F., Yu-Chen Lin, A., Andy Hong, P.K., 2011. Sorption and

636 biodegradation of sulfonamide antibiotics by activated sludge: Experimental
637 assessment using batch data obtained under aerobic conditions. *Water Res.* 45, 3389–
638 3397. <https://doi.org/10.1016/j.watres.2011.03.052>
639
640